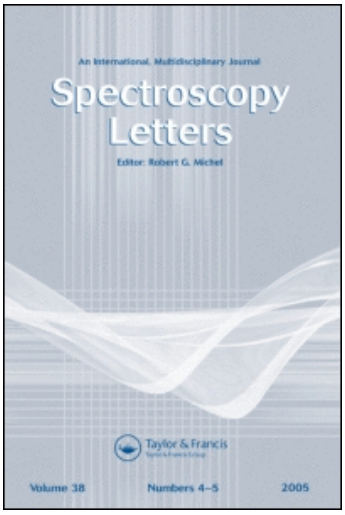

Spectroscopy Letters
Publication details, including instructions for authors and subscription information:
http://www.informaworld.com/smpp/title~content=t713597299

Self-Aggregation Behavior of *meso*-Tetra-(4-trimethylaminophenyl)porphyrin Encapsulated in Reverse Micelles

Nuo Zhang[a]; Yang Xia[a]; Dan Wu[a]; Ru Li[a]; Hongmin Ma[a]; Bin Du[a]; Qin Wei[a]
[a] School of Chemistry and Chemical Engineering, University of Jinan, Jinan, China

Online publication date: 27 April 2010

To cite this Article Zhang, Nuo , Xia, Yang , Wu, Dan , Li, Ru , Ma, Hongmin , Du, Bin and Wei, Qin(2010) 'Self-Aggregation Behavior of *meso*-Tetra-(4-trimethylaminophenyl)porphyrin Encapsulated in Reverse Micelles', Spectroscopy Letters, 43: 4, 275 — 281
To link to this Article: DOI: 10.1080/00387010903334540
URL: http://dx.doi.org/10.1080/00387010903334540

Spectroscopy Letters, 43:275–281, 2010

ISSN: 0038-7010 print/1532-2289 online
DOI: 10.1080/00387010903334540

Taylor & Francis
Taylor & Francis Group

Self-Aggregation Behavior of *meso*-Tetra-(4-trimethylaminophenyl)porphyrin Encapsulated in Reverse Micelles

Nuo Zhang,
Yang Xia,
Dan Wu,
Ru Li,
Hongmin Ma,
Bin Du,
and Qin Wei

School of Chemistry and Chemical Engineering, University of Jinan, Jinan, China

ABSTRACT The aggregation behavior of cationic *meso*-tetra-(4-trimethylaminophenyl)porphyrin (TAPP) was investigated in two reverse micelles (RM) of ionic surfactants, cetyltrimethylammonium bromide (CTAB) and bis(2-ethylhexyl)sulfosuccinate (AOT) using absorption spectroscopy, fluorescence spectroscopy, and resonance light scattering spectroscopy. TAPP showed different types of aggregation upon varying the ratio of water concentration to CTAB concentration, ω_0. The charge on the surfactant used to form reverse micelles determines the aggregation of porphyrin. The addition of hydrochloric acid can transform the H-aggregates of TAPP into monomers, while the addition of sodium hydroxide led to J-aggregation. Ionic strength had no significant influence on the aggregation of TAPP.

KEYWORDS aggregation, *meso*-tetra-(4-trimethylaminophenyl)porphyrin, reverse micelles, spectroscopy

INTRODUCTION

In recent years, porphyrins and their analogs with supramolecular functions have shown great potential in their recent application to various fields.[1–4] For example, they can be used as therapeutic drugs or photosensitizers for cancer detection and photodynamic therapy.[5–6] However, porphyrins are usually introduced into the blood stream as relatively concentrated solutions which can result in diminished activity, or adverse effects due to spontaneous aggregation processes.[7] Although porphyrin aggregates play specific roles in photosynthetic plants and organisms,[8] the processes behind their formation and possible effects in the human body are not fully understood. In-depth comprehension of the effect of porphyrins and metalloporphyrins in cells and the human body therefore requires a study of the aggregation behavior in a system that closely resembles the biological intracellular environment.

The self-assembly of different surfactant molecules into organized micelle structures with unique morphologies and dimensions, provides a good cellular simulation system. Reverse micelles (RM) are stable dispersions of water in nonpolar solvents and have been used extensively as biological

Received 15 August 2009;
accepted 14 September 2009.

Address correspondence to Qin Wei, School of Chemistry and Chemical Engineering, University of Jinan, Jinan 250022, Shandong Province, China. E-mail: sdjndxwq@163.com

membrane models to aid in the understanding of membrane chemistry.[9–11] Thus, RM can also provide a suitable simulation environment to study the aggregation of porphyrins in cells.

The charge on porphyrin derivatives significantly impacts its interaction with the bio-target molecule as well as the photodynamic efficiency. The positively charged porphyrins themselves are photosensitizers for photodynamic therapy and aggregate easily in cultured cells. There are many methods that can be used to investigate the aggregation behavior of porphyrin, such as absorption spectroscopy,[12] fluorescence spectroscopy[13,14] and resonance light scattering spectroscopy.[15] Determination of the position and shape of the Soret bands allow us to distinguish between monomeric porphyrins and various types of aggregates. Depending on the geometrical arrangement of the chromophores, the exciton theory developed by Kasha[16] predicts the occurrence of hypsochromic or bathochromic shifts for the relevant absorption bands, in the case of H-type (face-to-face) or J-type (side-by-side) interactions, respectively. The fluorescence spectroscopy is an important auxiliary method to study the aggregation of porphyrins. Using the resonance light scattering spectroscopy to investigate the porphyrin aggregation is an excellent method. If there are aggregates existed, the resonance light scattering signal is very strong. Therefore, extended aggregation is evaluated by resonance light scattering. In the present study, we extend our work on self-aggregation of porphyrins in aqueous solution to RM in an attempt to better understand and control the potential aggregation processes in real human cells. The structure of TAPP is shown in Fig. 1.

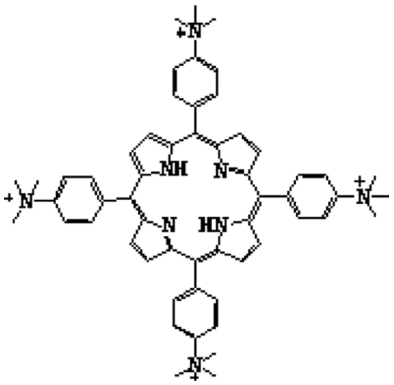

FIGURE 1 Structure of TAPP.

EXPERIMENTAL

Apparatus

A Perkin-Elmer Lambda-35 UV-Vis spectrophotometer with a 2 nm slit and 480 nm/min scanning velocity was used for all UV-visible absorption measurements. Fluorescence measurements were recorded with a Perkin–Elmer LS-55 fluorescence spectrometer. Band-pass slits of 15 and 6 nm were used for fluorescence excitation and emission monitoring of TAPP respectively. The excitation wavelength was set at 412 nm. The fluorescence spectra were scanned from 610 to 780 nm with a scanning velocity of 500 nm/min. The resonance light scattering spectra were obtained by using synchronous excitation and emission scanning with right-angle geometry, corrected by subtracting the corresponding blank sample. Band-pass slits of 15 and 2.5 nm were used for excitation and 2.5 nm for TAPP excitation and emission monitoring respectively. The scan resonance scattering spectrum ranged from 350 to 600 nm with a 500 nm/min scanning velocity. KQ-100E ultrasonic cleaner (Kunshan City Ultrasonic Instrument Co., Ltd., Kunshan City, China) was used to prepare CTAB and AOT reverse micelles. PeakFit data processing software was used to fit the data to the absorption spectrum.

Reagents

CTAB RM solutions were prepared by adding double-distilled water into the CTAB/isobutanol/n-octane mixture and shaking for a few seconds until a transparent solution was obtained. In the experiment, the entire volume injected was considered as water and used to calculate ω_0 ($\omega_0 = [H_2O]/[CTAB]$). TAPP was synthesized in-house at this laboratory. The concentration of TAPP was determined spectrophotometrically considering the molar extinction coefficient, $\varepsilon_{412nm} = 4.16 \times 10^5\,L \cdot mol^{-1} \cdot cm^{-1}$.

RESULTS AND DISCUSSION

The Aggregation of TAPP in CTAB RM at Variable ω_0

Figure 2 displays the absorption spectra of TAPP at different ω_0. At low water content ($\omega_0 \leq 12$), there are two peaks in the absorbance spectra, so we think

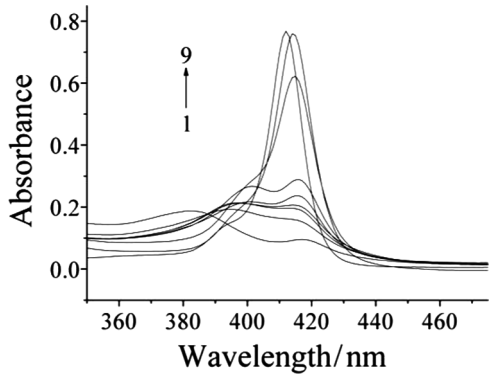

FIGURE 2 **Absorption spectra of TAPP encapsulated in CTAB RM at different ω_0. Curves: 1 ~ 9: ω_0 = 3, 4, 5, 6, 8, 12, 20, 30, aqueous solution; [TAPP] = 1.84×10^{-6} mol·L^{-1}.**

that there are multiple species of aggregates and monomers present. The absorption peaks located at 382 to 402 nm indicated the existence of H-aggregates. Upon increasing ω_0, H-aggregates converted into monomers. At higher water content ($\omega_0 \geq 20$), the absorption spectra of TAPP were similar to those for the aqueous solution. As the water content increased up to $\omega_0 = 30$, we assume that most of the TAPP molecules were in monomer form. Moreover, no isosbestic point was found, indicating the existence of multiple species in CTAB RM (H-aggregates species were different) and more than one distribution equilibrium between H-aggregates and monomers. Figures 3 and 4 verified the conclusion that increasing the ω_0 gradually converted H-aggregates into monomers.

The formation of porphyrin aggregates may lead to difficult interlaminar electron energy radiation, which can make the value of fluorescence quantum yield decrease. Therefore, the fluorescence intensity of porphyrin decreased. As shown in Fig. 3, when

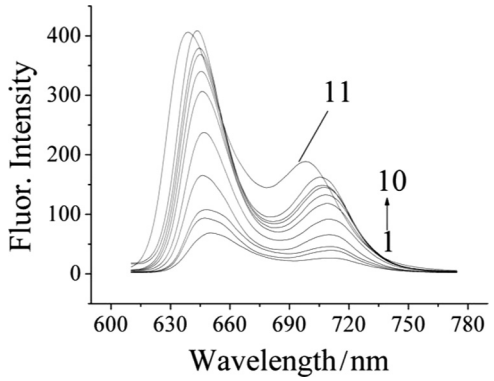

FIGURE 3 **Fluorescence spectra of TAPP with different ω_0 in CTAB RM. Curves 1 ~ 11: ω_0 = 3, 5, 6, 8, 10, 12, 14, 16, 20, 30, aqueous solution; [TAPP] = 1.84×10^{-6} mol·L^{-1}.**

the water decreases to $\omega_0 = 12$, obvious fluorescence quenching occurs, which indicated the existence of aggregation. The figure also shows that upon increasing ω_0, two well-defined emission bands always existed and their intensity gradually increased as they shifted to the blue with peaks changing from 648 and 714 nm to 643 and 705 nm, respectively, but still red-shifted relative to those obtained in free water. Based on the spectroscopic data one would be tempted to assign the major component at lower ω_0 to the H-aggregate responsible for absorption below 402 nm.

Resonance light scattering technique is an effective method to detect porphyrin aggregates. Due to the strong electronic coupling between chromogenic groups, the resonance light scattering signal is enhanced greatly at the maximum absorption wavelength. As shown in Fig. 4, the intensity of resonance light generally diminishes as ω_0 increases, indicating the conversion of H-aggregates into monomers. We could also see that $\omega_0 = 12$ was a critical value. At low water content ($\omega_0 \leq 12$), the intensity of resonant light was relatively large. The maximum of resonance light scattering peak was located at about 391 nm. The spectral shape between 350 and 400 nm had significant differences from that obtained in water. This further indicated the existence of H-aggregates.

When the radius of the RM was small and the enclosed volume contained very little water, there were significant differences between the aqueous solution inside and outside of the RM. One possible explanation for this is that the water molecules inside the RM were fixed to the inner wall. When the radius of the RM increased, the number of free water molecules would also increase, and the properties of the water inside the RM would more closely reflect those of the free aqueous solution. RM has the ability to solubilize large amounts of water, forming spherical monodisperse droplets that do not vary with dispersed-phase volume fraction or temperature.[17] The entrapped water influences the RM radius, shape, and polar headgroup packing. Therefore, the parameter ω_0 used to describe these systems is directly proportional to the micellar radius.[18] FTIR and NMR spectroscopy indicate that water solubilized inside small micelles ($\omega_0 \leq 7$) was bound to the polar headgroups of AOT, thus inhibiting their ability to form hydrogen bonds as found in bulk water.[19,20] Solvation dynamics also shows that water

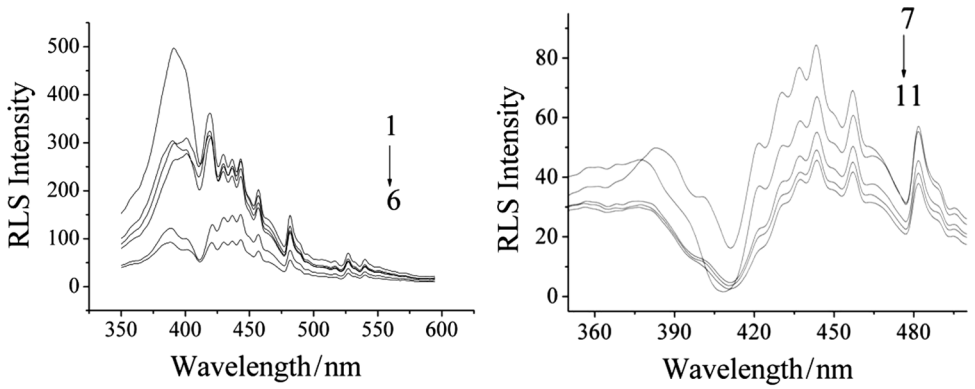

FIGURE 4 RLS spectra of TAPP with different ω_0 in CTAB RM. (a) Curves 1 ~ 6: ω_0 = 3, 5, 6, 8, 10, 12; [TAPP] = 1.84×10^{-6} mol·L^{-1}; (b) Curves 7 ~ 11: ω_0 = 14, 16, 20, 30, aqueous solution; [TAPP] = 1.84×10^{-6} mol·L^{-1}.

inside the smallest micelles is immobilized, but a bulk-like component appears as water is added and a water core forms.[21]

The cations of CTAB repel TAPP because of its positive charge. Furthermore, because of the small volume within these RM, spatial confinement effects also lead to H-aggregates via $\pi-\pi$ stacking interactions. We also investigated the aggregation of TAPP at different ω_0 in AOT RM and found there were no aggregates even when ω_0 was reduced to 3. It is speculated that this result was related to the negative charge of AOT. The negative charge could result in the binding of TAPP onto the inner wall of AOT RM in the form of a monomer. The continued reduction of ω_0 inhibited the solubilization of TAPP, resulting in delamination. A similar trend was also observed in two water-soluble freebase porphyrins: negatively charged *meso*-tetrakis(p-sulfonatophenyl)-porphyrin sodium salt (TSPP) and positively charged *meso*-tetrakis(N-methylpyridinium-4-yl)-porphyrin (TMpyP).[14]

The Effect of Strong Acid Medium on the Aggregation of TAPP in CTAB RM

The effect of hydrochloric acid on the aggregation behavior of TAPP in CTAB RM at water content $\omega_0 = 20$ was studied, and the results are shown in Fig. 5. At relatively low acidity, the absorbance of TAPP increased with increasing acidity. This may be caused by H-aggregates' disaggregation into monomers. When the concentration of HCl was 3.09×10^{-5} mol·L^{-1}, the spectra showed an increase in the Soret band maximum from 414 to 438 nm followed by a concomitant red-shift. Four Q-bands also notably changed upon further increases of the acidity, among which Q_y (1, 0) and Q_y (0, 0) bands disappeared,

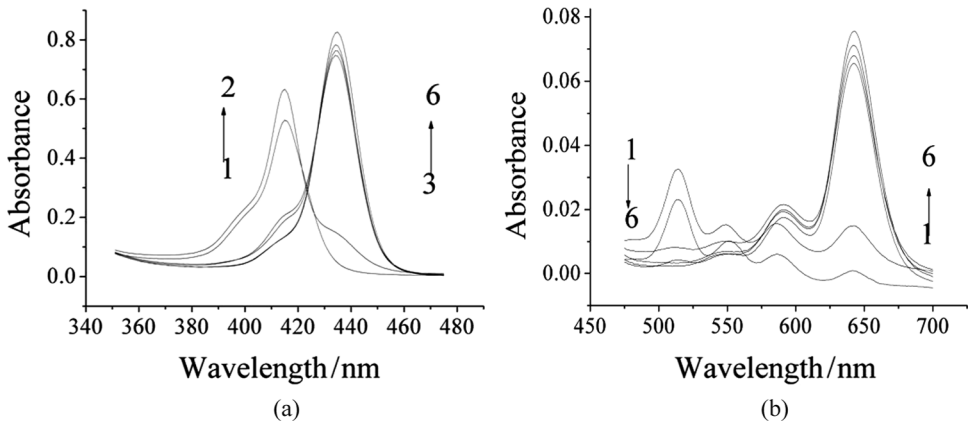

FIGURE 5 Absorption spectra of TAPP with different concentrations of HCl in CTAB RM. (a) B band of curves 1 ~ 6; (b) Q bands of curves 1 ~ 6; Curves: 1 ~ 6: [HCl] = 9.65×10^{-6} mol·L^{-1}, 1.93×10^{-5} mol·L^{-1}, 3.09×10^{-5} mol·L^{-1}, 9.65×10^{-5} mol·L^{-1}, 9.65×10^{-4} mol·L^{-1}, 1.93×10^{-3} mol·L^{-1}; [TAPP] = 1.84×10^{-6} mol·L^{-1}.

while the absorbance of Q_x (1, 0) and Q_x (0, 0) increased, with the latter increasing significantly.

Under similar experimental conditions, the fluorescence spectra and resonance light scattering spectra were obtained for TAPP in CTAB RM, as displayed in Fig. 6. Fluorescence quenching occurred with the shape of the spectrum changing when the concentration of HCl was $3.09 \times 10^{-5}\,\mathrm{mol \cdot L^{-1}}$. When the concentration of HCl increased to $9.65 \times 10^{-4}\,\mathrm{mol \cdot L^{-1}}$, the two fluorescence emission peaks changed into one peak significantly red-shifted from 642 to 662 nm. The resonance scattering spectrum also changed significantly with the increasing acidity at HCl concentration of $3.09 \times 10^{-5}\,\mathrm{mol \cdot L^{-1}}$. Maximum scattering as well as the wave valley both experienced red shifts from 443 to 456 nm, and 410 to 431 nm, respectively.

Judging from the absorption spectra, fluorescence spectra and resonance scattering spectra, TAPP apparently formed into a porphyrin diacid because of protonation with increasing acidity, but there were no signs of aggregation appearing. The positive charge on TAPP increased, enhancing the repulsion between TAPP within the CTAB RM and reducing TAPP's potential to form aggregates.

The Effect of Strong Alkali Medium on the Aggregation of TAPP in CTAB RM

The effect of sodium hydroxide on the aggregation behavior of TAPP in CTAB RM at water content $\omega_0 = 20$ was also studied.

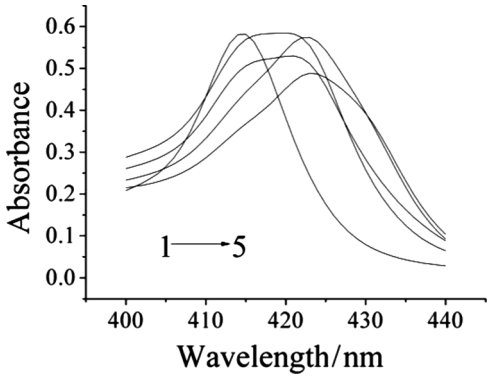

FIGURE 7 B band of TAPP with different concentrations of NaOH. Curves $1 \sim 5$: $[NaOH] = 1.93 \times 10^{-4}\,\mathrm{mol \cdot L^{-1}}$, $9.65 \times 10^{-4}\,\mathrm{mol \cdot L^{-1}}$, $1.93 \times 10^{-3}\,\mathrm{mol \cdot L^{-1}}$, $3.86 \times 10^{-3}\,\mathrm{mol \cdot L^{-1}}$, $5.79 \times 10^{-3}\,\mathrm{mol \cdot L^{-1}}$; $[TAPP] = 1.84 \times 10^{-6}\,\mathrm{mol \cdot L^{-1}}$.

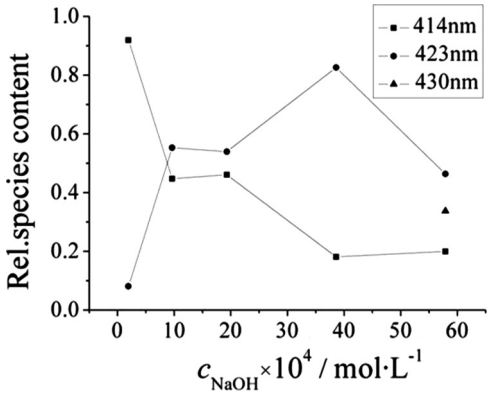

FIGURE 8 The effect of concentrations of NaOH on the Rel. species content of TAPP.

As shown in Fig. 7, the Soret band of the absorption spectra red shifted from 414 to 423 nm upon increasing the NaOH concentration. Our preliminary conclusion is that there were J-aggregates. We used

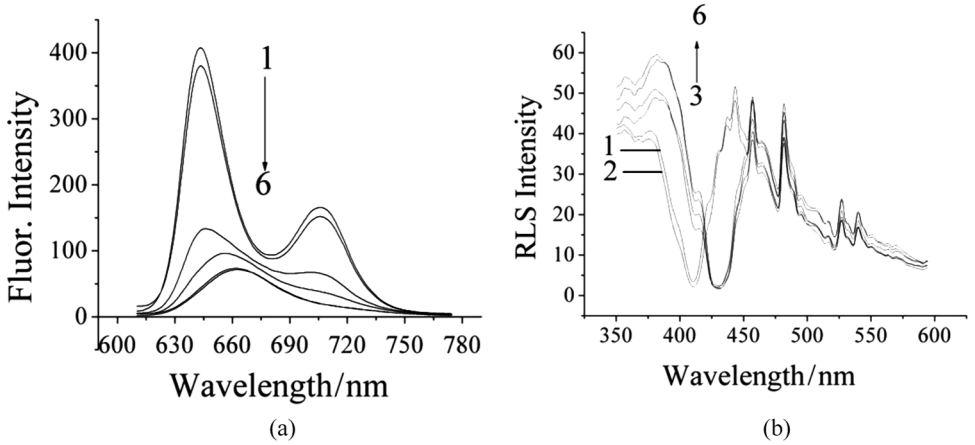

FIGURE 6 Fluorescence spectra (a) and RLS spectra (b) of TAPP with different concentrations of HCl in CTAB RM. Curves: $1 \sim 6$: $[HCl] = 9.65 \times 10^{-6}\,\mathrm{mol \cdot L^{-1}}$, $1.93 \times 10^{-5}\,\mathrm{mol \cdot L^{-1}}$, $3.09 \times 10^{-5}\,\mathrm{mol \cdot L^{-1}}$, $9.65 \times 10^{-5}\,\mathrm{mol \cdot L^{-1}}$, $9.65 \times 10^{-4}\,\mathrm{mol \cdot L^{-1}}$, $1.93 \times 10^{-3}\,\mathrm{mol \cdot L^{-1}}$; $[TAPP] = 1.84 \times 10^{-6}\,\mathrm{mol \cdot L^{-1}}$.

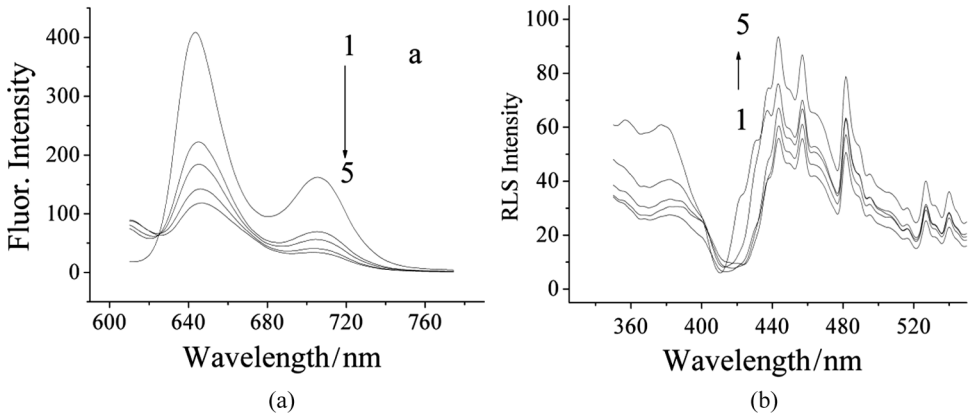

FIGURE 9 Fluorescence spectra (a) and RLS Spectra (b) of TAPP with different concentrations of NaOH. Curves 1 ~ 5: [NaOH] = 1.93×10^{-4} mol·L^{-1}, 9.65×10^{-4} mol·L^{-1}, 1.93×10^{-3} mol·L^{-1}, 3.86×10^{-3} mol·L^{-1}, 5.79×10^{-3} mol·L^{-1}; [TAPP] = 1.84×10^{-6} mol·L^{-1}.

PeakFit data processing software to fit data to the absorption spectrum and the results are presented in Fig. 8.

Figure 8 shows TAPP's transformation from monomer to J-aggregate form with absorption peaks at 414 and 423 nm, respectively. When the concentration of NaOH reached a threshold value, TAPP could also form more complicated J-aggregate species with an absorption peak at 430 nm. Using similar experimental conditions, the fluorescence spectra and resonance scattering spectra were measured for TAPP in CTAB RM, as shown in Fig. 9, which further verified our conclusions.

Figure 9a shows fluorescence quenching with the fluorescence emission peaks at 642 and 702 nm gradually widening, and the absorption spectrum red shifting with the increase in NaOH. Figure 9b shows the intensity of resonance light increasing significantly with the increase of NaOH. Considering these results, we judged that the addition of NaOH caused TAPP to form J-aggregates. So we could speculate that strong NaOH condition would influence the existing form of TAPP. At high NaOH concentrations, the nitrogen in the pyrrole ring undergoes a deprotonation process, causing OH^- groups to migrate to the interior of the RM and bind to its inner wall.

The Effect of Ionic Strength on the Aggregation of TAPP in CTAB RM

At different water contents, the ionic strength did not significantly influence the aggregation of TAPP. The electrostatic repulsion between cationic porphyrins was very strong. In addition, the positively charged nitrogens in the pyrrole rings bonded with three methyls, and the large volume of these peripheral groups increased steric hindrance. Changes in the ionic strength alone cannot cause TAPP aggregation.

CONCLUSIONS

The aggregation behavior of cationic porphyrin TAPP was studied in CTAB cationic reverse micelles. The water content, ω_0, determined the RM radius[16] and influenced the properties of water within the RM, thus affecting TAPP aggregation behavior. When $\omega_0 \leq 12$, water was bound to the inner wall of the RM. In this situation, coexistence of H-aggregates and monomers was found. TAPP existed in form of monomer only in large RM when the water content was high, and free water molecules were present. After studying the aggregation behavior of TAPP in AOT RM and referencing the pertinent literature, we inferred that the charge on the surfactant forming the reverse micelle had decisive influence on porphyrin aggregation. Water-soluble cationic porphyrin could aggregate in cationic reverse micelles, but not in anionic reverse micelles. Moreover, the addition of HCl could cause TAPP to form porphyrin diacid species, promoting transformation from H-aggregates to monomer form. The addition of NaOH causes TAPP to undergo a deprotonation process leading to J-aggregation. Different ionic strength had no significant influence on the existing form of TAPP.

ACKNOWLEDGMENTS

This study was supported by the Natural Science Foundation of China (20577016), the Natural Science

Foundation of Shandong Province (Y2006B36 and Y2008B44) and the Key Subject Research Foundation of Shandong Province (XTD0705), and all the authors express their deep thanks.

REFERENCES

1. Lehn, J. M. Perspectives in supramolecular chemistry-from molecular recognition towards molecular information processing and self-organization. *Angew. Chem. Int. Ed.* **1990**, *29*(11), 1304–1319.
2. Komagoe, K.; Tamagake, K.; Katsu, T. The influence of aggregation of porphyrins on the efficiency of photogeneration of hydrogen peroxide in aqueous solution. *Chem. Pharm. Bull.* **2006**, *54*(7), 1004–1009.
3. Mosinger, J.; Janošková, M.; Lang, K.; Kubát, P. Light-induced aggregation of cationic porphyrins. *J. Photoch. Photobio. A* **2006**, *181*, 283–289.
4. Agarwal, N. The synthesis and characterization of photonic materials composed of substituted fluorene donors and a porphyrin acceptor. *Dyes Pigments* **2009**, *83*, 328–333.
5. Macdonald, I. J.; Dougherty, T. J. Basic principles of photodynamic therapy. *J. Porphyrins. Phthalocyanines* **2001**, *5*, 105–129.
6. Ogawa, K.; Hasegawa, H.; Inaba, Y.; Kobuke, Y.; Inouye, H.; Kanemitsu, Y.; Kohno, E.; Hirano, T.; Ogura, S.; Okura, I. Water-soluble bis(imidazolylporphyrin) self-assemblies with large two-photon absorption cross sections as potential agents for photodynamic therapy. *J. Med. Chem.* **2006**, *49*, 2276–2283.
7. Keene, J. P.; Kessel, D.; Land, E. J.; Redmond, R. W.; Truscott, T. G. Direct detection of singlet oxygen sensitized by haematoporphyrin and related compounds. *Photochem. Photobiol.* **1986**, *43*(2), 117–120.
8. White, W. I. *The Porphyrins*; Academic Press: New York, 1979, Chapter 7.
9. Luisi, P. L.; Giomini, M.; Pileni, M. P.; Robinson, B. H. Reverse micelles as hosts for proteins and small molecules. *Biochim. Biophys. Acta* **1988**, *947*, 209–246.
10. Andrade, S. M.; Costa, S. M. B.; Pansu, R. The influence of water on the photophysical and photochemical properties of piroxicam in AOT/isooctane/water reversed micelles. *Photochem. Photobiol.* **2000**, *71*(4), 405–412.
11. Andrade, S. M.; Costa, S. M. B.; Pansu, R. Structural changes in w/o Triton X-100//cyclohexane-hexanol/water microemulsions probed by a fluorescent drug piroxicam. *J. Colloid Interface Sci.* **2000**, *226*(2), 260–268.
12. Kubát, P.; Lang, K.; Procházková, K.; Anzenbacher, P. Jr. Self-aggregates of cationic meso-Tetratolylporphyrins in aqueous solutions. *Langmuir* **2003**, *19*, 422–428.
13. Mizutani, T.; Wada, K.; Kitagawa, S. Porphyrin receptors for amines, amino acids, and oligopetides in water. *J. Am. Chem. Soc.* **1999**, *121*, 11425–11431.
14. Andrade, S. M.; Costa, S. M. B. Spectroscopic studies of water-soluble porphyrins with protein encapsulated in bis(2-ethylhexyl) sulfosuccinate (AOT) reverse micelles: aggregation versus complexation. *Chem. Eur. J.* **2006**, *12*(4), 1046–1057.
15. Pasternack, R. F.; Bustamante, C.; Collings, P. J.; Giannetto, A.; Gibs, E. J. Porphyrin assemblies on DNA as studied by a resonance light-scattering technique. *J. Am. Chem. Soc.* **1993**, *115*(13), 5393–5399.
16. Kasha, M.; Rawls, H. R.; El-Bayoumi, M. A. The exciton model in molecular spectroscopy. *Pure Appl. Chem.* **1965**, *11*, 371–392.
17. Kunieda, H.; Shinoda, K. Solution behavior of aerosol OT/water/oil system. *J. Colloid Interface Sci.* **1979**, *70*, 577–583.
18. Zulauf, M.; Eicke, H. F. Inverted micelles and microemulsions in the ternary system H_2O/aerosol-OT/isooctaneas studied by photon correlation spectroscopy. *J. Phys. Chem.* **1979**, *83*(4), 480–486.
19. Christopher, D. J.; Yarwood, J.; Belton, P. S.; Hills, B. P. A Fourier transform infrared study of water-head group interactions in reversed micelles containing sodium (2-ethylhexyl) sulfosuccinate (AOT). *J. Colloid Interface Sci.* **1992**, *152*(2), 465–472.
20. Christenson, H.; Friberg, S. E.; Larsen, D. W. NMR investidations of aggredation of nonionic surfactants in a hydrocarbon medium. *J. Phys. Chem.* **1980**, *84*(26), 3633–3638.
21. Faeder, J.; Ladanyi, B. M. Molecular dynamics simulations of the interior of aqueous reverse micelles. *J. Phys. Chem. B* **2000**, *104*, 1033–1046.